Quantum Chemical Calculation of Excited States of Flavin-Related Molecules

Christian Neiss,[†] Peter Saalfrank,*[,†] Maja Parac,[‡] and Stefan Grimme[‡]

Institut für Physikalische und Theoretische Chemie, Universität Regensburg, Universitätsstrasse 31, D-93053 Regensburg, Germany, and Organisch-Chemisches Institut, Westfälische Wilhelms-Universität Münster, Corrensstrasse 40, D-48149 Münster, Germany

Received: July 19, 2002; In Final Form: October 24, 2002

The performance of various methods of various quantum mechanical methods for the calculation of low-lying singlet and triplet excited states of biologically relevant species related to flavins is critically examined. In particular, configuration interaction singles (CIS), time-dependent density functional theory (TD-DFT), and the recently proposed multireference configuration interaction DFT method (DFT/MRCI) [Grimme, S.; Waletzke, M. *J. Chem. Phys.* **1999**, *111*, 5645] are compared. For the DFT-based methods, various hybrid exchange−correlation functionals are used. For the "test molecule" uracil, it is found that CIS does not give quantitatively accurate energies even in conjunction with large basis sets including diffuse functions. In contrast TD-DFT(B3LYP) and DFT/MRCI produce reasonably accurate results even with medium-sized basis sets such as 6-31G*. Following these test calculations, the absorption energies of the lumiflavin molecule in its ground (i.e., $S_0 \rightarrow S_n$) and lowest triplet state (i.e., $T_1 \rightarrow T_n$) are investigated. The nature of the low-lying excited states is discussed, and the results are compared to experiment. Finally, the effect of surrounding water molecules and of geometrical distortions on the absorption spectrum of flavin-type species is discussed on the basis of model calculations.

1. Introduction

Flavins play an important role for many enzymological reactions. The basic structure of the flavin family, from which all other variants derive, is 7,8-dimethyl-10-methyl-isoalloxazine, which is also called lumiflavin (see Figure 1). Related species are riboflavin, FMN (flavin mononucleotide), and FAD (flavin adenine dinucleotide), in which the methyl group at N10 is replaced by a sugar chain, sugar plus phosphate group, and sugar plus phosphate plus nucleotide base, respectively. These species act as prosthetic groups in many proteins, most frequently catalyzing redox reactions. Flavoenzymes are also known as central for light-mediated signal transduction. For example, in the blue-light photoreceptor phototropin,[1] the photoexcitation of flavin is the initial step of a subsequent, long reaction cascade.

In general, the understanding of photoactive pigments requires knowledge of the absorption spectrum of the central chromphore, that is, excitation energies, oscillator strenghts, and lifetimes of the excited states. From a theoretical point of view, this is a challenge for a number of reasons. First, the light-active molecules such as flavins are not small. Second, more than only a few excited states may be of importance. Third, the molecules bind to proteins, which are often the key to their biological relevance. Finally, the molecules are not in the gas phase but rather embedded in an environment, for example, water.

In the past, several calculations on flavin-type molecules have been carried out. Most of them dealt with the (singlet or triplet or both) electronic ground state; the adopted methods used range from semiempirical[2−4] to Hartree−Fock[5−7] theory and hybrid density functional theory.[8] For the excited states of flavins, relevant for their photochemistry and -physics, only rather old calculations by Song et al.[9,10] using the Pariser−Parr−Pople/configuration interaction (PPP/CI) method and semiempirical calculations at the complete neglect of differential overlap/configuration interaction singles (CNDO/CIS) level of theory are available.[11] According to these calculations, the lowest visible absorption bands can be attributed to $\pi \rightarrow \pi^*$ transitions; but, while the PPP method was able to reproduce the experimentally found spectra quite well in terms of position and intensity of the absorption bands, the newer CNDO/CIS results compare less favorably with experiment. Moreover, according to our knowledge, there are no theoretical spectra concerning excitation from the lowest triplet state of flavin available despite the fact that the triplet absorption spectrum has been known experimentally for a long time, see, for example, ref 12.

In an ongoing effort to model the photoexcitation and subsequent reactions of flavin-type molecules in phototropin by quantum mechanical techniques,[13] we are interested in theoretical methods that are at the same time sufficiently "accurate" and reasonably "cheap". It is also our goal to go beyond the semiemprical theory for the excited states of flavin-type molecules, as mentioned above. The requirement of "accuracy" is met by standard ab initio methods such as (multireference) configuration interaction [(MR)CI], coupled cluster (CC) theory, and complete active space perturtbation theory (e.g., CASPT2),[14,15] to name but a few. However, these methods are rarely "cheap" at least if one goes beyond the more simple CI singles (CIS) level of theory. Recently, methods based on density functional theory (DFT) were found attractive in terms of accuracy and computational effort. This holds true not only for ground states but also for electronically excited states. The most prominent example is the time-dependent DFT (TD-DFT) method,[16] in which excited-state properties are determined from the linear response of the molecules to an external continuous wave field. Yet another approach combines CI-type

[†] Universität Regensburg.
[‡] Westfälische Wilhelms-Universität Münster.

10.1021/jp021671h CCC: $25.00
Published on Web 12/04/2002

ideas with Kohn−Sham (KS) DFT. An example is the DFT/single excitation configuration interaction (SCI) method,[17] in which the Kohn−Sham (rather than Hartree−Fock) orbital energies are used along with empirically adjusted two-electron integrals. This method works well for the absorption spectra of larger molecules provided single excitations dominate and the ground state can be accurately represented by a single determinant. For more general situations, a multireference description which also includes static correlation is to be preferred; consequently, a DFT/MRCI method was proposed,[18] which proved successful when applied to excited states of organic molecules, for example.

In this paper, we perform a series of calculations for several flavin-related molecules (uracil, isolumazine, lumiflavin), using various methods: CIS, TD-DFT, and DFT/MRCI. One aim is to understand and interpret the experimental absorption spectra (if available) and to study the dependence of selected electronic transitions on the size of the molecule, its geometrical structure, and its environment. Another goal is to address the performance of the above-mentioned methods for this class of biologically relevant species. In addition, comparisons to previous calculations will be made where possible.

The paper is organized as follows. In the next section, the theoretical methods and their computational realization will be described in brief. In section 3.1, we will test the performance of the CIS and TD-DFT(B3LYP) methods in combination with a great variety of basis sets when applied to uracil, which serves as a "test molecule". In the sections 3.2 and 3.3, the CIS, TD-DFT, and DFT/MRCI methods will be used and compared for the calculation of singlet and triplet excited states of lumiflavin and isolumazine. The effects of molecular structure and a water environment will be discussed. Section 4 summarizes and concludes this work.

2. Methods and Computational Details

Prior to calculating excited states, all molecules were geometry-optimized in their ground state on the B3LYP/6-31G* level of theory using the Gaussian 98 program;[19] closed-shell molecules were treated with the restricted method and open-shell triplet states by the unrestricted formalism (UB3LYP). It should be mentioned that the UB3YLP method is known to be very robust against spin contamination.[20] The minimum geometries were confirmed by a frequency analysis. Also the stability of the wave function was checked. The computational models used for the excited states are CIS,[21] TD-DFT,[16] and DFT/MRCI.[18]

In the well-known CIS method single excitations out of a Hartree−Fock (HF) reference determinant are used together with two-electron integrals built from HF orbitals to construct the CI matrix.

In the TD-DFT method, linear response theory is adopted to calculate excitation energies and oscillator strengths as the poles and residues, respectively, of the frequency-dependent molecular (mean) polarizability. In the following, we use the KS-DFT in conjunction with the hybrid B3LYP exchange−correlation functional,[22] if not stated otherwise.

For both the CIS and the TD-DFT(B3LYP) calculations, the Gaussian 98[19] program is used. While CIS gives only rather crude estimates for the excited states, it is known that TD-DFT in conjunction with hybrid functionals can be quite accurate.[23,24]

If multiple excitations and multideterminant effects contribute significantly to an excited state (i.e., if the usual adiabatic approximation in TD-DFT breaks down), a multireference description that also accounts for static correlation is more appropriate. Moreover, the most popular ab initio methods for that purpose become impractical to handle if the number of correlated electrons is large. The combined density functional theory/multireference configuration interaction (DFT/MRCI) method by Grimme and Waletzke has proven to give accurate electronic spectra of organic molecules.[18,25] In this approach, the basic idea is to include major parts of dynamic correlation by density functional theory, and the nondynamical part of the correlation energy, which cannot be described adequately by the functionals available nowadays, is recovered by short MRCI expansions. An effective Hamiltonian in a basis of spin- and space-symmetry-adapted configuration state functions (CSF), which are built up from Kohn−Sham (KS) orbitals, is used to calculate the configuration interaction (CI) wave function for the electronic state of molecules. The diagonal elements of the effective DFT/MRCI Hamiltonian are constructed from an exact Hartree−Fock-based expression and a DFT-specific correction term. For the off-diagonal elements of the CI matrix, an empirical, energy-dependent scaling is employed. In the DFT/MRCI Hamiltonian, five empirical parameters are employed. At present, optimized parameters are usable only for Becke's "half-and-half" hybrid exchange−correlation functional (BH-LYP).[18] Computationally costly four-index integrals in the MO basis are evaluated semidirectly using the well-known resolution of the identity (RI) method[26,27] and employing the RI-MP2 optimized auxiliary basis sets from the TURBOMOLE library.[28] For more details, we refer to the original paper.[18]

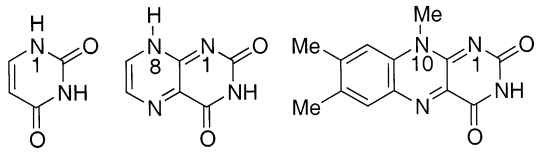

Figure 1. Structure formulas of uracil (left), isolumazine (middle), and lumiflavin (right) with numbering of the ring N atoms indicated.

All oscillator strengths used in this paper were calculated in the dipole length representation. Basis sets will be specified below. The computer platforms used are Linux-based Intel Pentium III and AMD Athlon machines.

3. Results and Discussion

3.1. Excited States of Uracil. The pyrimidine base uracil ($C_4N_2O_2H_4$), Figure 1, is taken as a simple model system for flavins to test the performance of the methods and various basis sets. This molecule is chosen because it is structurally related to flavins but is still sufficiently small to allow for a systematic study. Furthermore, there are numerous experimental spectra to compare with.

The CIS and TD-DFT(B3LYP) methods were used in conjunction with basis sets ranging from rather small without polarization or diffuse functions (6-31G, 80 basis functions) up to aug-cc-pVTZ[29,30] (460 basis functions) to calculate the 10 lowest singlet and the 10 lowest triplet excited states above the B3LYP/6-31G* geometry-optimized singlet ground state. In addition, the performance of the DFT/MRCI method in conjunction with the SV(P) basis[31] is tested. The results are presented in Tables 1 and 2.

As already mentioned, a large number of experimental spectra are available for uracil, most of them, however, in solvents such as water. In this case typically, a structureless absorption band with maximum at approximately 260 nm (ca. 38 500 cm^{-1} or 4.77 eV) is reported and a second one at 210 nm (ca. 47 600 cm^{-1} or 5.90 eV).[32] For other solvents, such as chloroform ($CHCl_3$) and 1,4-dioxane ($C_4H_8O_2$), the longer-wavelength

TABLE 1: Vertical Lowest CIS Excitation Energies (in eV; some states are omitted) of Uracil for Different Basis Sets at the B3LYP/6-31G* Optimized Geometry[a]

	CIS				
	/6-31G*	/6-31+G*	/cc-pVTZ	/aug-cc-pVTZ	expt
$1^1A' \rightarrow 1^3A'$	3.44	3.44	3.44	3.43	
$\rightarrow 2^3A'$	5.68	5.70	5.72	5.72	
$\rightarrow 1^3A''$	5.71	5.75	5.74	5.74	
$\rightarrow 1^1A''$	6.29	6.32	6.33	6.32	
$\rightarrow 2^1A'$	**6.67**	**6.49**	**6.47**	**6.35**	**5.08**
⋮	⋮	⋮	⋮	⋮	
$\rightarrow 3^1A'$	**8.62**	**8.20**	**8.47**	**8.19**	**6.05**
basis functions	128	160	296	460	
time	12 min	26 min	14 h 52 min	102 h 32 min	

[a] The times given refer to the total computation time on a PIII 733 MHz computer. Also, the corresponding experimental values are indicated.[34]

absorption feature is slightly blue-shifted to 254 nm (ca. 39 400 cm^{-1} or 4.88 eV).[33] Also, gas-phase spectra were reported.[34,35] Unfortunately, these appear to be broad as well with an overall shape similar to those in solution, albeit further blue-shifted: the long-wavelength absorption band is found at 244 nm (ca. 41 000 cm^{-1} or 5.08 eV) with a weak shoulder at 205 nm (ca. 48 800 cm or 6.05 eV), and the short-wavelength band appears at 187 nm (ca. 53 500 cm^{-1} or 6.63 eV).

Our results in Tables 1 (CIS) and 2 (DFT methods) indicate that the CIS excitation energies are always higher than those computed with TD-DFT(B3LYP) and DFT/MRCI, independent of the basis set. Only the lowest triplet $1^3A'$ is essentially the same for both methods (ca. 3.4 eV) and refers to the spin-forbidden HOMO−LUMO ($\pi \rightarrow \pi^*$) transition (see Figure 2). The spin-allowed HOMO−LUMO ($1^1A' \rightarrow 2^1A'$) transition corresponds to the lowest visible transition of uracil (experimentally at 5.08 eV, see above). The computed data depend sensitively on the method used. From Table 1, we note that the corresponding CIS excitation energy is, even with the best basis set (aug-cc-pVTZ), too high by about 1.3 eV (∼6.35 eV). In contrast, the TD-DFT(B3LYP) excitation energy is 5.11 eV and

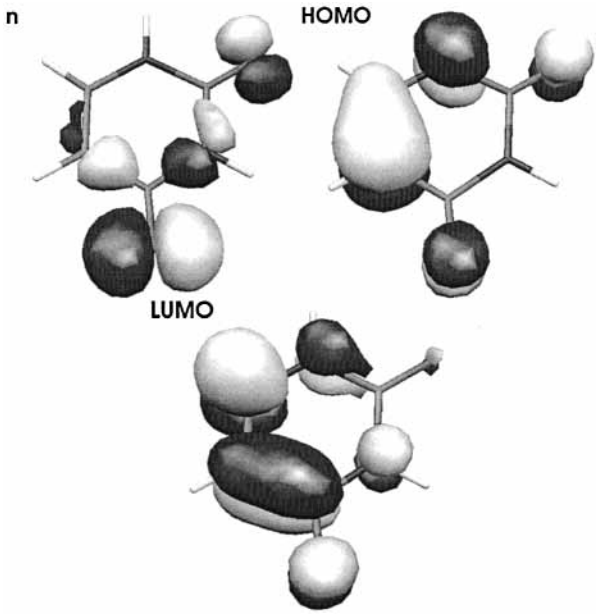

Figure 2. Most important orbitals for the lowest $A' \rightarrow A'$ ($1^1A' \rightarrow 2^1A'$) and $A' \rightarrow A''$ ($1^1A' \rightarrow 1^1A''$) transitions of uracil (see text).

therefore in good agreement with experiment. The observation of CIS overestimating excitation energies is qualitatively due to the neglect of most electron correlation effects. Regarding the DFT/MRCI method, it can be stated that the results are comparable to those of TD-B3LYP, however, with the DFT/MRCI code being much more efficient (in Table 2, the approximate CPU times are indicated).

It is further found that the energetic position of the first excited state, $2^1A'$, is shifted upward, that is, away from experiment, if smaller basis sets are used. For CIS, the basis-set-related blue shift is quite substantial and amounts to an additional 0.32 eV error when going from aug-cc-pVTZ to 6-31G*. For TD-DFT(B3LYP), the corresponding blue shift is only ∼0.20 eV. For other states, the basis-set dependence of

TABLE 2: Vertical TD-DFT(B3LYP) and DFT/MRCI Excitation Energies (in eV) of Uracil for Different Basis Sets at the B3LYP/6-31G* Optimized Geometry[a]

	TD-DFT(B3LYP)									DFT/MRCI	
	/6-31G	/6-311G	/SV(P)	/6-31G*	/6-31G**	/6-31+G*	/cc-pVDZ	/cc-pVTZ	/aug-cc-pVTZ	/SV(P)	expt
$1^1A' \rightarrow 1^3A'$	3.43	3.44	3.34	3.42	3.42	3.42	3.42	3.40	3.38	3.66	
$\rightarrow 1^3A''$	4.23	4.25	4.24	4.27	4.25	4.32	4.23	4.27	4.26	4.25	
$\rightarrow 1^1A''$	4.65	4.67	4.65	4.67	4.66	4.71	4.63	4.66	4.64	4.45	
$\rightarrow 2^3A'$	4.67	4.67	4.73	4.74	4.74	4.75	4.71	4.73	4.71	4.97	
$\rightarrow 2^1A'$	**5.31**	**5.28**	**5.31**	**5.31**	**5.30**	**5.20**	**5.27**	**5.20**	**5.11**	**5.48**	**5.08**
$\rightarrow 3^3A'$	5.33	5.34	5.46	5.43	5.43	5.37	5.44	5.41	5.74	5.74	
$\rightarrow 2^3A''$	5.50	5.51	5.52	5.55	5.54	5.57	5.49	5.53	5.49	5.71	
$\rightarrow 3^3A''$*	6.99	6.27	6.53	6.90	6.93	5.37	6.43	6.23	5.58	6.87	
$\rightarrow 2^1A''$*	7.21	6.42	6.70	7.13	7.15	5.75	6.60	6.37	5.64	7.03	
$\rightarrow 3^1A''$	5.81	5.81	5.79	5.82	5.81	5.83	5.76	5.78	5.74	5.90	
$\rightarrow 3^1A'$	**6.01**	**5.98**	**5.98**	**5.99**	**5.98**	**5.93**	**5.92**	**5.91**	**5.85**	**6.06**	**6.05**
$\rightarrow 4^3A'$	5.85	5.86	5.94	5.94	5.93	5.91	5.92	5.93	5.87	6.28	
$\rightarrow 4^3A''$	6.01	6.01	6.04	6.04	6.03	6.04	6.00	6.02	5.96	6.46	
$\rightarrow 4^1A''$	6.17	6.18	6.22	6.22	6.21	6.19	6.19	6.20	6.12	6.51	
$\rightarrow 5^3A'$(*)				7.69	7.69	6.41			6.25	7.75	
$\rightarrow 4^1A'$(*)		7.13	7.37			6.27	7.28	7.08	6.27		
$\rightarrow 5^3A''$	6.38	6.39	6.44	6.47	6.46	6.43	6.44	6.44	6.37	6.79	
$\rightarrow 5^1A'$	**6.63**	**6.60**	**6.72**	**6.68**	**6.68**	**6.51**	**6.68**	**6.56**	**6.39**	**6.81**	**6.63**
$\rightarrow 6^1A'$	7.62		7.37	7.65	7.65		7.65			7.60	
basis functions	80	116	1220	128	140	160	132	296	460	120	
time	1 h 15 min	2 h 15 min	2 h 52 min	3 h 26 min	3 h 53 min	6 h 23 min	7 h 17 min	27 h 03 min	140 h 14 min	∼0 h 5 min	

[a] The times given refer to the total computation time using a parallel two-processor PIII 700 MHz Computer. Where no value is given, no corresponding state could be found; ∗ labels states with a very strong basis-set dependence. States that dominate the spectrum in Figure 3 are indicated in bold. Experimental values are taken from ref 34.

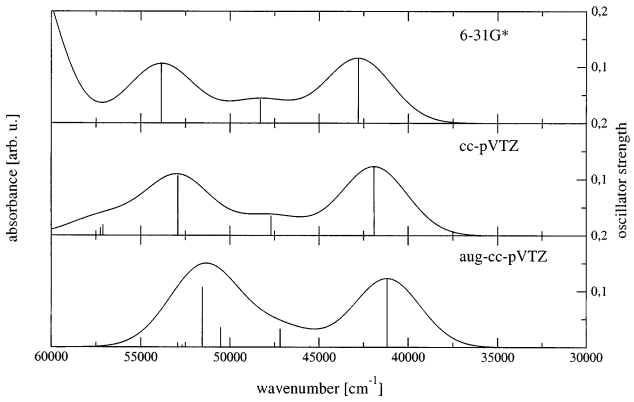

Figure 3. Absorption spectra for uracil computed with TD-DFT-(B3LYP) and different basis sets. Both the line spectra and the artificially broadened spectra are shown (see text). The oscillator strengths of the computed transitions (lines) are also given.

the excitation energies is typically smaller, both for TD-DFT and CIS. There are a few exceptions to this rule when the basis-set dependence becomes quite strong, see below.

Below the just mentioned $1^1A' \rightarrow 2^1A'$ transition, there is another spin-allowed transition, $1^1A' \rightarrow 1^1A''$, corresponding to $n \rightarrow \pi^*$ (see Figure 2). The corresponding oscillator strength (intensity), however, is smaller by a factor of about 10^3 than that for the HOMO−LUMO transition and therefore not visible. Also all other $^1A' \rightarrow {}^1A''$ transitions have very small oscillator strengths and are therefore hidden under the more intense $^1A' \rightarrow {}^1A'$ absorption features. To quantify this, in Figure 3, simulated absorption spectra calculated with TD-DFT(B3LYP) are shown for three different basis sets. The simulated spectra are obtained by broadening the theoretical line spectra with Gaussians:

$$I(\tilde{\nu}) \sim \sum_i f(i)\, \mathrm{e}^{-1/2((\tilde{\nu}-\tilde{\nu}_i)/\sigma)^2} \qquad (1)$$

Here $\sigma = 1300$ cm^{-1} is the width of the Gaussians centered at peak number i with wavenumber $\tilde{\nu}_i$ and oscillator strength $f(i)$. This procedure roughly accounts for the finite experimental resolution and vibrational and rotational broadening, finite lifetime, and nonvertical transition effects.

Referring to the lowest panel of the figure (aug-cc-pVDZ), we already assigned the strongest low-energy peak $1^1A' \rightarrow 2^1A'$ at 5.11 eV (41 200 cm^{-1}) to the HOMO−LUMO transition, which is experimentally found at 41 000 cm^{-1} (5.08 eV). The weak shoulder observed at about 48 800 cm^{-1} (or 6.05 eV) appears to be mostly due to the $1^1A' \rightarrow 3^1A'$ transition at about 47 200 cm^{-1} (5.85 eV) in Table 2 (aug-cc-pVTZ basis), which is dominated by the HOMO-2 → LUMO one-electron excitation. The experimental intense high-energy peak at about 53 500 cm^{-1} (6.63 eV) is assigned to the $1^1A' \rightarrow 5^1A'$ transition at around 51 500 cm^{-1} (6.39 eV) in Table 2, which is due to the excitation of an electron out of the HOMO into a higher-lying π-orbital. Those final states that dominate the spectrum in Figure 3 are indicated in bold in Table 2. We conclude that the TD-DFT-(B3LYP) absorption spectrum is in good agreement with experiment.

By comparing the different panels of Figure 3, we note the above-mentioned blue shift of the spectra when basis sets of decreasing quality are used. However, the shift is comparably small, and the overall spectral features are quite insensitive to the basis set at least if only the low-energy part of the spectrum is concerned. This is of great practical importance because according to Table 2 the computational effort of the TD-DFT-(B3LYP) method scales approximately with the third power of the number of basis functions in the present application. Hence, we conclude that for larger molecules of the flavin-type already a relatively small basis set such as 6-31G* gives reasonably accurate results. From the table, however, we also note that there are several states (indicated by asterisks) the exact positions of which depend sensitively on the quality of the basis set. In particular, diffuse functions are required for these states indicating that they are of Rydberg-like character. Fortunately, these states do not contribute substantially to the absorption spectrum of uracil up to about 7 eV (∼56 500 cm^{-1}).

3.2. Excited States of Lumiflavin. Next, we discuss the flavin prototype molecule lumiflavin (cf. Figure 1). In particular, we are interested in the absorption spectra of the singlet ground state (S_0) and of the lowest triplet state (T_1), which both can be compared to experiment. Both states have been discussed in connection with their biological relevance—the T_1, for example, for its reactivity with amino acids.[36]

Again, we adopt the CIS and the TD-DFT methods, and we compare these to DFT/MRCI. For the CIS calculation, the 6-31G* basis set is used; for DFT/MRCI, we adopt the SV(P) basis, which is of similar quality. As mentioned above, for DFT/MRCI, we use the BHLYP exchange−correlation functional. To systematically assess the effects of different basis sets and of different exchange−correlation functionals, the TD-DFT calculations are carried out with the two basis sets 6-31G* and SV(P) and the two functionals B3LYP and BHLYP. The geometries of the ground state, S_0, and the lowest triplet state, T_1, are the respective optimized (U)B3LYP/6-31G* geometries, which are found to be very similar.

3.2.1. Excitation out of the S_0 State. In Table 3, excitation energies are given for the S_0 ground state, as obtained with the CIS/6-31G*, TD-DFT(B3LYP)/6-31G*, TD-DFT(B3LYP)/SV-(P), TD-DFT(BHLYP)/SV(P), and DFT/MRCI/SV(P) methods (for CIS, only a few selected values are shown).

We first note from the table that the CIS method predicts once more consistently (by up to more than 1 eV) larger excitation energies than the DFT-based methods. As will be argued below, the DFT-based methods agree much better with experiment. Second, when comparing TD-DFT(B3LYP)/6-31G* and TD-DFT(B3LYP)/SV(P), we find that both basis sets are of almost equal quality, as expected. Third, the TD-DFT-(B3LYP) and DFT/MRCI methods give very similar results—deviations among them are rarely larger than 0.2 eV, in many cases smaller than 0.1 eV. The fact that two quite different methods to calculate excited states agree well supports confidence in the results.

It must be noted, however, that the TD-DFT(B3LYP) and TD-DFT(BHLYP) methods deviate substantially from each other (sometimes by more than 1 eV). This is obviously due to the higher portion of Hartree−Fock exchange in the BHLYP functional (50%) compared to the B3LYP functional (20%). Because CIS overestimates the excitation energies by more than 1 eV, one could expect errors of $\gtrsim$0.5 eV in the TD-DFT-(BHLYP) case; the B3LYP functional represents obviously a good compromise when used with time-dependent theory. However, DFT/MRCI results with the BHLYP functional are of good accuracy, which can be attributed to the multireference character of the wave function used.

The computed oscillator strengths indicate that only $A' \rightarrow A'$ transitions will be visible, while $A' \rightarrow A''$ are typically much weaker. This is in full analogy with uracil. Note, however, that the two lowest excited singlet states above S_0 are, in energetic

TABLE 3: Excitation Energies out of the S_0 Ground State of Lumiflavin (in eV; some states are omitted) as Obtained with Different Methods[a]

	CIS /6-31G*	TD-DFT(B3LYP) /6-31G*	TD-DFT(B3LYP) /SV(P)	TD-DFT(BHLYP) /SV(P)	DFC/MRCI /SV(P)	expt
$1^1A' \rightarrow 1^3A'$	2.41	2.07	2.07	1.96	2.23	
$\rightarrow 1^3A''$	3.61	2.76	2.70	3.09	2.86	
$\rightarrow$ **$2^1A'$**	**4.33**	**3.04**	**3.04**	**3.51**	**2.96**	**2.78**
$\rightarrow 2^3A'$	3.35	2.84	2.85	2.66	3.08	
$\rightarrow 2^3A''$		2.94	2.93	3.89	3.13	
$\rightarrow 2^1A''$	4.70	3.09	3.07	4.30	3.14	
$\rightarrow 1^1A''$		3.30	3.26	3.86	3.30	
$\rightarrow 3^3A'$		3.35	3.34	3.69	3.59	
$\rightarrow 3^3A''$		3.61	3.57	4.62	3.74	
$\rightarrow 4^3A'$		3.62	3.61	3.82	3.80	
$\rightarrow 3^1A''$		3.84	3.80	5.04	3.81	
$\rightarrow$ **$3^1A'$**	**5.19**	**3.86**	**3.87**	**4.38**	**3.90**	**3.35**
$\rightarrow 4^1A'$		4.00	3.99	5.12	4.05	
⋮	⋮	⋮	⋮	⋮	⋮	
$\rightarrow$ **$5^1A'$**	**6.09**	**4.91**	**4.72**	**5.42**	**4.89**	**4.59**

[a] Those states that dominate the spectrum in Figure 5 are indicated in bold. For CIS, only selected values are given. Experimental values are taken fom ref 37.

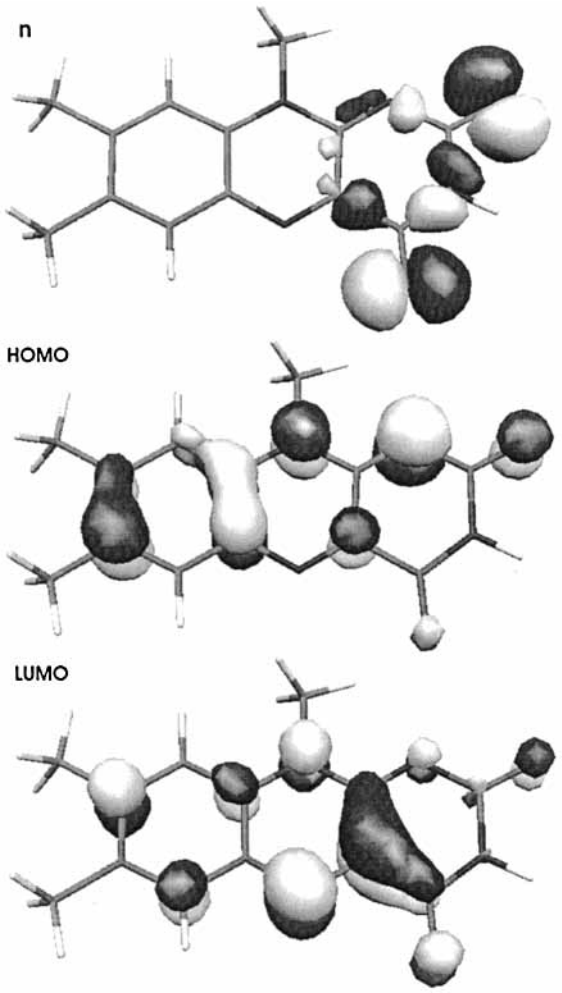

Figure 4. Most important orbitals for the lowest $A' \rightarrow A'$ and $A' \rightarrow A''$ transitions of lumiflavin (see text).

order, of A″ and A′ symmetry for lumiflavin, while for uracil, the ordering is reversed. Again, $1^1A' \rightarrow 2^1A'$ is dominated by the HOMO−LUMO transition ($\pi \rightarrow \pi^*$), while $1^1A' \rightarrow 1^1A''$ is of the $n \rightarrow \pi^*$ type by which electron density is transferred mainly from a nonbinding orbital to the LUMO, see Figure 4.

To the best of our knowledge, there are no published experimental gas-phase spectra of lumiflavin, riboflavin, or FMN. This is not very surprising in view of the low volatility

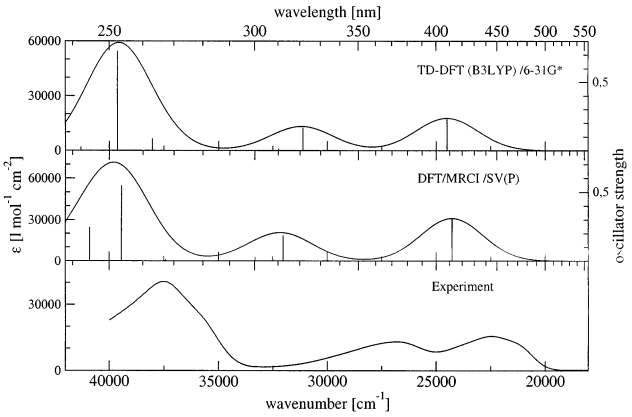

Figure 5. Calculated ground state (S_0) absorption spectra of lumiflavin obtained with two different methods. The spectra, and all the following ones, are broadened according to eq 1 with $\sigma = 1000$ cm^{-1}. The oscillator strengths for the computed transitions (lines) and the molar extinction coefficient ϵ for the experimental/calculated spectra are also given. The experimental spectrum refers to FMN diluted in water.[44]

of these species as compared to uracil. Thus, we refer to spectra recorded in solvents (mostly water) or of flavin embedded in proteins. In polar solvents such as water, lumiflavin shows two characteristic bands at 446 nm (ca. 22 400 cm^{-1} or 2.78 eV) and 370 nm (ca. 27 000 cm^{-1} or 3.35 eV), followed by a strong absorption band at 270 nm (37 000 cm^{-1} or 4.59 eV);[37] the corresponding spectra of riboflavin or FMN are practically identical. These data are very similar to the computed (and broadened) absorption spectra for (gas-phase) lumiflavin, which are shown and compared to the FMN spectrum in aqueous solution in Figure 5. For the DFT/MRCI spectrum, for example, we find three major peaks at around 24 000, 31 500, and close to 40 000 cm^{-1}, the last peak being the most intense. The dominant contributors to these peaks are indicated in Table 3 in bold. Given the fact that for uracil the absorption features of the gas-phase spectrum are blue-shifted by about 1200−2500 cm^{-1} (depending on which feature is considered) relative to the spectrum in (water) solution, the agreement between theory and experiment is very good. The same good agreement is also obtained with the TD-DFT(B3LYP) method (Figure 5, upper panel). In addition, the calculated oscillator strengths lead to extinction coefficients that are reasonably close to experiment, albeit the latter being somewhat larger than the former, see Figure 5.

Other experimental observations are also consistent with theory. For example, for FMN embedded in proteins or lumiflavin/riboflavin dissolved in ethanol at low temperatures (ca. 80K), additional vibrational fine structure in the absorption spectra have been reported[10,38,39] with fine structure peaks on top of the lowest electronic (HOMO → LUMO or $S_0 \rightarrow S_1$) transition separated by about 1300−1250 cm^{-1}. These additional peaks have been assigned to C−N and C−C stretching vibrations of the ring frame of lumiflavin.[40] Therefore, one would expect that the lowest visible transition is localized at the ring atoms as well. This is consistent with our calculations. By transfer of electron density from HOMO to LUMO, the bonding character between the ring atoms changes and primarily the above-mentioned vibrations are excited (see Figure 4). Because the lowest A′ → A′ transition is not localized in a small portion of the molecule, there is also only a small change in dipole moment from about 9.0 to 10.5 D (DFT/MRCI values). This is consistent with dipole measurements on FMN, FAD, and *N*(3)-methyl-*N*(10)-isobutyl-7,8-dimethyl-isoalloxazine by Stanley et al.,[38] who find that the S_1 state is more polar by about 1 D than the ground-state S_0. Moreover, the S_2 state is, according to their results, even more polar than the S_1; again, this is resembled by our calculations according to which the dipole moment is 14.2 D for S_2.

Comparing our TD-DFT or DFT/MRCI excited-state calculations to the semiempirical theory of Wouters et al.[11] and Song et al.,[9,10] respectively, we find that the former perform reasonably better than the latter. While the semiempirical methods are still reasonably accurate as far as the lowest absorption band is concerned, they appear to be less accurate for the higher-energy transitions. For CNDO/CIS, for example, the order of the higher-lying excited states seems to be reversed relative to our calculations and experiment. The PPP/CI theory seems to perform better for the second and higher absorption bands, but generally the PPP oscillator strengths seem to be somewhat inaccurate. For example, the oscillator strength of the lowest transition as reported by Song et al. is about 0.7, while we calculate a corresponding value of about 0.3, which seems to compare more favorably with experiment according to Figure 5.

3.2.2. Excitation out of the T_1 State. Experimental absorption spectra for T_1 of (nonprotonated) FMN or riboflavin, respectively, in aqueous solution or in a protein environment, were reported[41,42] and will be compared to our gas-phase calculations for lumiflavin, see Figure 6. The spectrum exhibits a broad band around 690 nm with two maxima at 715 nm (ca. 14 000 cm^{-1} or 1.73 eV) and 660 nm (ca. 15 200 cm^{-1} or 1.88 eV), which might be vibrational in nature,[42] followed by a weak peak/shoulder at 494 nm (ca. 20 200 cm^{-1} or 2.51 eV), a stronger band at 377 nm (ca. 26 500 cm^{-1} or 3.29 eV), and a very intense band at 270 nm (ca. 37 000 cm^{-1} or 4.59 eV). Apart from the more complicated structure, a major feature of the T_1 absorption spectrum as compared to S_0 is a strong red shift.

In Table 4, computed excitation energies out of the T_1 state of lumiflavin are listed. In Figure 6, the corresponding (broadened) absorption spectra are shown, which are found to be dominated by $^3A' \rightarrow {}^3A'$ transitions. Because of missing experimental extinction coefficients, only a qualitative comparison is possible.

Obviously, the model calculations account for the strong red shift of T_1 relative to S_0. The experimental spectrum is most closely resembled by the UTD-DFT(B3LYP) approach, but the theoretical absorption bands are still blue-shifted relative to experiment. The experimental spectrum, however, refers to flavin in water. The performance of the RTD-DFT(B3LYP) and DFT/MRCI methods appears less good when compared to the experimental curve. The RTD-DFT method shows also notedly higher oscillator strengths than the other two methods, see Figure 6; however, it should be noted that there might be a bug in the Gaussian 98 code for this case, because in newer versions of Gaussian 98 the calculation of transition densities between excited states (i.e., not involving the ground state) has been disabled because not all terms are correctly computed.[43] Indeed, as can be seen from Table 4, the different shapes of the theoretical spectra are mostly due to different oscillator strengths rather than different transition energies. For the UTD-DFT and DFT/MRCI method, the order of magnitude for the excitations is in the same range, at least.

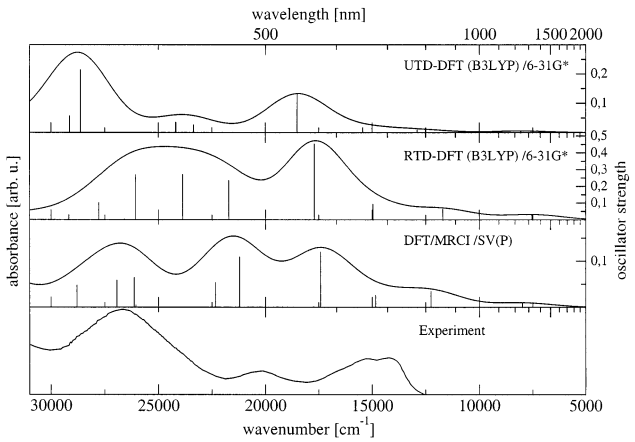

Figure 6. Calculated triplet (T_1) spectra of lumiflavin obtained with unrescricted and restricted TD-DFT(B3LYP) and the DFT/MRCI methods. For comparison, the experimental triplet spectrum of FMN in water is also shown (according to ref 41). Oscillator strengths refer to the computed transitions.

TABLE 4: Calculated Triplet Excitation Energies Starting from the Lowest Triplet State T_1 ($1^3A'$) of Lumiflavin[a]

	UTD-DFT(B3LYP) /6-31G*	RTD-DFT(B3LYP) /6-31G*	DFT/MRCI /SV(P)	expt
$1^3A' \rightarrow 2^3A'$	1.00	0.94	0.99	
$\rightarrow 1^3A''$	0.98	0.98	1.02	
$\rightarrow 2^3A''$	1.00	1.09	1.03	
$\rightarrow 3^3A'$	1.60	1.45	1.54	
$\rightarrow 3^3A''$	1.69	1.64	1.64	
$\rightarrow 4^3A'$	1.91	1.86	1.85	
$\rightarrow 5^3A'$	2.30	2.20	2.17	1.73, 1.88
$\rightarrow 4^3A''$	2.25	2.29	2.20	
$\rightarrow 6^3A'$	2.90	2.69	2.65	2.78
$\rightarrow 7^3A'$	3.00	2.96	2.79	
$\rightarrow 5^3A''$	3.26	3.11	3.13	
$\rightarrow 8^3A'$	3.55	3.23	3.25	3.29

[a] Only triplets were computed. Experimental values relate to triplet FMN in aqueous solution.[41]

The first strong absorption computed ($4^3A'$) is assigned to the above-mentioned experimental absorption band around 690 nm (1.80 eV). We notice that there are several lower-lying transitions, especially also of the A′ → A′ type, with rather small oscillator strenghts. However, these transitions are not visible in the experimental spectrum because of limitations of the setup: all experimental spectra end around 850 nm because of a rapid loss of spectral sensitivity of the detector above that wavelength. For the high-energy transitions, the computed oscillator strengths depend quite strongly on the particular method used, in contrast to the ground-state spectrum.

Other possible sources of deviations between theory and experiment are as follows: (1) The triplet spectrum may strongly depend on solvent effects. To investigate this possibility, we

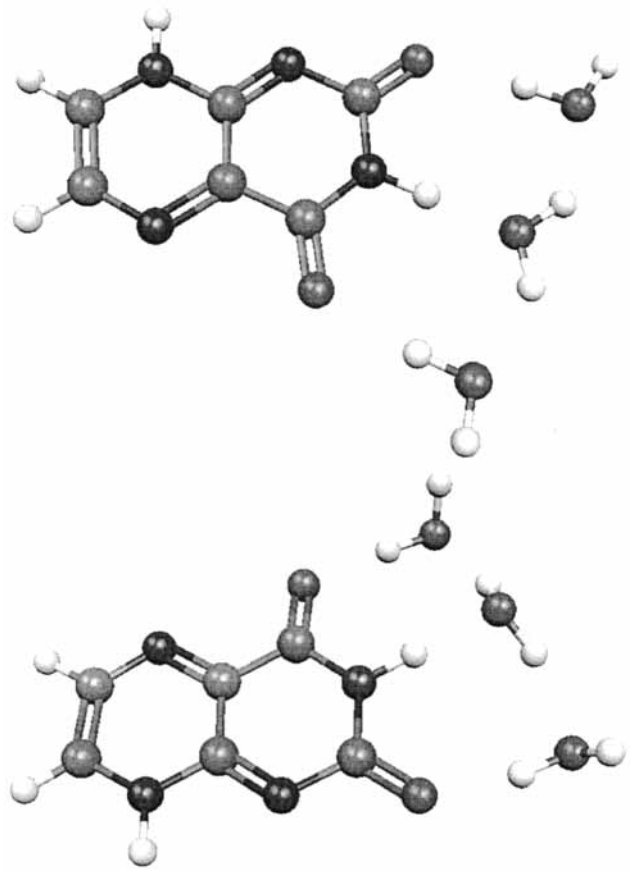

Figure 7. Optimized ground-state structures of isolumazine surrounded by three water molecules. Upper sketch refers to enforced C_s symmetry and the lower one to C_1 symmetry. The optimized triplet structures are very similiar and not shown here.

will study below the triplet absorption spectrum of the isolumazine molecule in the presence of (a few) water molecules. The isolumazine molecule serves as yet another computationally less-demanding model system for isolumazine. (2) It seems also possible that the spectrum is sensitive to changes of the molecular structure as possibly enforced by the solvent or the protein environment. This possibility will be discussed in subsection 3.3.2.

3.3. The Influence of an Environment on the Absorption Spectra of Flavin-type Molecules. *3.3.1. Isolumazine and the Effect of Solvent Molecules.* To test the influence of a solvent on the absorption spectra of flavin-type molecules in triplet and singlet states, we choose as a smaller model system for lumiflavin, the isolumazine molecule. Isolumazine derives from lumiflavin by removing the benzoid ring and replacing the methyl group at N10 with H, see Figure 1. The geometry of isolumazine was optimized at the B3LYP/6-31G* and UB3LYP/6-31G* levels of theory for the singlet S_0 and triplet T_1 states, respectively, and TD-DFT and DFT/MRCI calculations were carried out as before.

As a second model, three water molecules were added to those positions that are considered important also for hydrogen bonding in proteins. Again, a geometry optimization on the (U)-B3LYP/6-31G* level of theory was carried out, both for S_0 and T_1. The corresponding optimized structures are crude models for a "snapshot" of flavins in aqueous solution or of flavins in a protein environment. The optimal structure has C_1 symmetry and is shown, for the singlet, in the lower panel of Figure 7. We also considered another model system in which C_s symmetry was enforced as a constraint. The resulting constrained structure

TABLE 5: Calculated Singlet Excitation Energies (in eV) of Isolumazine and Isolumazine with Additional Water Molecules (see text) as Obtained with DFT/MRCI Method[a]

	TD-B3LYP	DFT/MRCI	DFT/MRCI ($3H_2O$, C_1 sym)	DFT/MRCI ($3H_2O$, C_s sym)
$1^1A' \rightarrow 1^1A''$	3.09	3.17	3.05	3.18
$\rightarrow$ **$2^1A'$**	**3.34**	**3.19**	**3.21**	**3.17**
$\rightarrow 2^1A''$	3.26	3.38	3.48	3.31
$\rightarrow 3^1A''$	3.91	3.94	4.02	4.00
$\rightarrow$ **$3^1A'$**	**4.01**	**4.09**	**4.10**	**3.86**
$\rightarrow 4^1A''$	4.58	4.66	4.49	4.69
$\rightarrow 5^1A''$	4.74	4.90	4.91	5.02
$\rightarrow$ **$4^1A'$**	**4.83**	**5.01**	**5.00**	**4.96**

[a] The corresponding TD-DFT(B3LYP) values for the water-free isolumazine are shown for comparison. Dominant transitions are indicated in bold.

TABLE 6: Calculated Singlet Excitation Energies (in eV) of Isolumazine and Isolumazine with Additional Water Molecules (see text) as Obtained with DFT/MRCI Method[a]

	UTD-B3LYP	DFT/MRCI	DFT/MRCI ($3H_2O$, C_1 sym)	DFT/MRCI ($3H_2O$, C_s sym)
$1^3A' \rightarrow 1^3A''$	1.04	1.10	0.97	
$\rightarrow 2^3A''$	1.11	1.19	1.23	
$\rightarrow$ **$1^3A'$**	**1.66**	**1.61**	**1.56**	**1.46**
$\rightarrow 3^3A''$	1.75	1.81	1.84	
$\rightarrow 2^3A'$	2.05	2.05	2.04	2.04
$\rightarrow 4^3A''$	2.39	2.43	2.28	
$\rightarrow$ **$3^3A'$**	**2.63**	**2.64**	**2.58**	**2.60**
$\rightarrow$ **$4^3A'$**	**3.17**	**3.13**	**3.06**	**3.11**

[a] The corresponding TD-DFT(B3LYP) values for the water-free isolumazine are shown for comparison. Dominant transitions are indicated in bold.

serves as a model for a second instantaneous configuration of flavin in water (upper panel of Figure 7). Of course, this model is very simple because in reality many water molecules are present and an average over all possible configurations will be necessary. Nevertheless, basic trends may become visible. The different configurations were then used for calculating excited states within the TD-DFT and DFT/MRCI methods.

The computed singlet excitation energies from the S_0 state are shown in Table 5. The left two panels refer to the water-free spectra for the TD-DFT and DFT/MRCI methods, which are again quite similar. When adding water molecules in the C_1 and C_s configurations and using the DFT/MRCI method, we find as a major effect a small red shift of the main spectral features. For the C_s configuration, the red shift is about 400 wavenumbers for the most intense peak centered slightly above 40 000 cm^{-1} ($1^1A' \rightarrow 4^1A'$) and about 100 cm^{-1} for the low-energy peak around 26 000 cm^{-1} ($1^1A' \rightarrow 2^1A'$). The biggest effect is on $1^1A' \rightarrow 3^1A'$ (which is remarkably weaker than that in isolumazin), for which a red shift of about 1900 cm^{-1} is observed.

The observed red shift in a water "environment" is consistent with the experimental findings for uracil. There, however, the absolute shifts are larger, which is easily attributed to the fact that only a few water molecules have been considered in the computational model.

The computed triplet spectra for isolumazine are shown in Table 6. The triplet spectra are not much more influenced by the water molecules than the singlet spectra. Again, a red shift occurs, with the low-energy peak around 1300 cm^{-1} being lowered by the largest amount (a few hundred wavenumbers). The red shift goes in the right direction as far as agreement between theory and experiment is concerned (see Figure 6). The

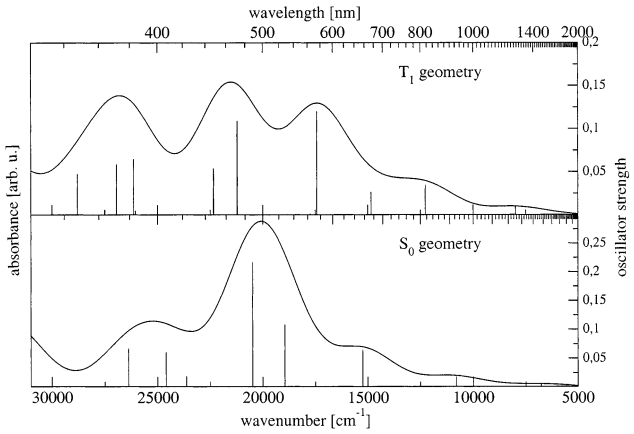

Figure 8. Calculated triplet absorption spectra of lumiflavin as obtained by the DFT/MRCI method with either T_1 or S_0 ground-state geometry. Oscillator strengths refer to the computed transitions.

order of the transitions and their relative intensities remain largely unaffected.

3.3.2. The Role of Geometrical Distortions. Another factor that might be important for quantitative comparison of experiment and theory is the possible geometrical distortion of the molecule enforced by an environment. In particular, when the molecule is embedded in a protein cavity, subtle geometrical changes occur. One may further speculate that these rearrangements are quantitatively different for singlets and triplets.

To address the effect of geometry distortions on triplet spectra of flavin-type molecules, both the isolumazine and lumiflavin molecules were considered. We performed caclulations on the DFT/MRCI/SV(P) level of theory. The (water-free) triplet spectra had been computed with the UB3LYP/6-31G*-optimized geometries for the respective T_1 state. As a model for distorted molecules, we repeat the same calculation starting, however, from the B3LYP/6-31G* geometry that was optimized for the S_0 state.

For the lumiflavin molecule, the two calculated spectra are compared in Figure 8. Despite the fact that the optimized T_1 and S_0 geometries are, at first glance, quite similar, the geometrical differences are sufficient to cause substantial changes. Similar changes are also observed for the triplet spectrum of isolumazine (not shown). It is therefore concluded that geometrical distortions of the chromophore by an environment may have a distinct influence on the spectra.

4. Conclusions

In this work, we have shown that it is possible to compute ground-state absorption spectra and properties of excited states of flavins with good accuracy by using the TD-DFT(B3LYP) or DFT/MRCI methods with moderately large basis sets. In contrast, the CIS method is not only inferior in terms of accuracy (even with very large basis sets) but also not much cheaper than the DFT-based methods used here. Also, preliminary calculations of how to go beyond the isolated-molecule approach have been presented. This work opens the way for the application of the present methodology to calculate excited states and absorption spectra and (photo-) reactions of flavins in a (natural) environment; work along these lines is in progress in our laboratory.

Acknowledgment. Fruitful discussions with B. Dick are gratefully acknowledged. This work was supported by the Deutsche Forschungsgemeinschaft within the Graduiertenkolleg "Sensory photoreceptors in natural and artificial systems" (GK640/1).

References and Notes

(1) Crosson, S.; Moffat, K. *Proc. Natl. Acad. Sci. U.S.A.* **2001**, *98*, 2995.
(2) Hall, L. H.; Orchard, B. J.; Tripathy, S. K. *Int. J. Quantum Chem.* **1987**, *31*, 195.
(3) Hall, L. H.; Orchard, B. J.; Tripathy, S. K. *Int. J. Quantum Chem.* **1987**, *31*, 217.
(4) Hall, L. H.; Bowers, M. L.; Durfor, C. N. *Biochemistry* **1987**, *26*, 7401.
(5) Platenkamp, R. J.; Palmer, M. H.; Visser, A. J. W. G. *Eur. Biophys. J.* **1987**, *14*, 393.
(6) Meyer, M.; Hartwig, H.; Schomburg, D. *J. Mol. Struct. (THEOCHEM)* **1996**, *364*, 139.
(7) Zheng, Y.-J.; Ornstein, R. L. *J. Am. Chem. Soc.* **1996**, *118*, 9402.
(8) Meyer, M. *J. Mol. Struct. (THEOCHEM)* **1997**, *417*, 163.
(9) Song, P.-S. *Int. J. Quantum Chem.* **1969**, *3*, 303.
(10) Sun, M.; Moore, T. A.; Song, P.-S. *J. Am. Chem. Soc.* **1972**, *94*, 1730.
(11) Wouters, J.; Durant, F.; Champagne, B.; André, J.-M. *Int. J. Quantum Chem.* **1997**, *64*, 721.
(12) Tegnér, L. *Photochem. Photobiol.* **1966**, *5*, 223.
(13) Neiss, Ch.; Saalfrank, P. *Photochem. Photobiol.*, in press.
(14) Szabo, A.; Ostlund, N. S. *Modern Quantum Chemistry: Introduction to Advanced Electronic Structure Theory*; Macmillan Publishing Co., Inc.: New York, 1982.
(15) Jensen, F. *Introduction to Computational Chemistry*; John Wiley & Sons: New York, 1999.
(16) Gross, E.; Dobson, J.; Petersilka, M. *Top. Curr. Chem.* **1996**, *181*, 81.
(17) Grimme, S. *Chem. Phys. Lett.* **1996**, *259*, 128.
(18) Grimme, S.; Waletzke, M. *J. Chem. Phys.* **1999**, *111*, 5645.
(19) Frisch, M. J.; Trucks, G. W.; Schlegel, H. B.; Scuseria, G. E.; Robb, M. A.; Cheeseman, J. R.; Zakrzewski, V. G.; Montgomery, J. A., Jr.; Stratmann, R. E.; Burant, J. C.; Dapprich, S.; Millam, J. M.; Daniels, A. D.; Kudin, K. N.; Strain, M. C.; Farkas, O.; Tomasi, J.; Barone, V.; Cossi, M.; Cammi, R.; Mennucci, B.; Pomelli, C.; Adamo, C.; Clifford, S.; Ochterski, J.; Petersson, G. A.; Ayala, P. Y.; Cui, Q.; Morokuma, K.; Malick, D. K.; Rabuck, A. D.; Raghavachari, K.; Foresman, J. B.; Cioslowski, J.; Ortiz, J. V.; Stefanov, B. B.; Liu, G.; Liashenko, A.; Piskorz, P.; Komaromi, I.; Gomperts, R.; Martin, R. L.; Fox, D. J.; Keith, T.; Al-Laham, M. A.; Peng, C. Y.; Nanayakkara, A.; Gonzalez, C.; Challacombe, M.; Gill, P. M. W.; Johnson, B. G.; Chen, W.; Wong, M. W.; Andres, J. L.; Head-Gordon, M.; Replogle, E. S.; Pople, J. A. *Gaussian 98*, revision A.7; Gaussian, Inc.: Pittsburgh, PA, 1998.
(20) Woeller, M.; Grimme, S.; Peyerimhoff, S.; Danovich, D.; Filatov, M.; Shaik, S. *J. Phys. Chem. A* **2000**, *104*, 5366.
(21) Foresman, J. B.; Head-Gordon, M.; Pople, J. A. *J. Phys. Chem.* **1992**, *96*, 135.
(22) Becke, A. *J. Chem. Phys.* **1993**, *98*, 5648.
(23) Bauernschmitt, R.; Ahlrichs, R. *Chem. Phys. Lett.* **1996**, *256*, 454.
(24) Stratmann, R. E.; Scuseria, G.; Frisch, M. J. *J. Chem. Phys.* **1998**, *109*, 8218.
(25) Parusel, A. B. J.; Grimme, S. *J. Porphyrins Phthalocyanins* **2001**, *5*, 225.
(26) Vahtras, O.; Almlöf, J.; Feyereisen, M. W. *Chem. Phys. Lett.* **1993**, *213*, 514.
(27) Weigend, F.; Häser, M. *Theor. Chem. Acc.* **1997**, *97*, 331.
(28) Weigend, F.; Häser, M.; Patzelt, M. H.; Ahlrichs, R. *Chem. Phys. Lett.* **1998**, *294*, 143.
(29) Woon, D. E.; Dunning, T. H. J. *J. Chem. Phys.* **1993**, *98*, 1358.
(30) Kendall, R. A.; Dunning, T. H. J. *J. Chem. Phys.* **1992**, *96*, 6796.
(31) Schäfer, A.; Horn, H.; Ahlrichs, R. *J. Chem. Phys.* **1992**, *97*, 2751.
(32) Iza, N.; Gil, M.; Morcillo, J. *J. Mol. Struct.* **1999**, *175*, 31.
(33) Masoud, M.; Ahmed, A.; Ahmed, R. *Pak. J. Sci. Ind. Res.* **1999**, *42*, 11.
(34) Clark, L. B.; Peschel, G.; Tinoco, I. *J. Phys. Chem.* **1965**, *69*, 3615.
(35) Brady, B. B.; Peteanu, L. A.; Levy, D. H. *Chem. Phys. Lett.* **1988**, *147*, 538.
(36) Heelis, P.; Parsons, B.; Phillips, G.; McKellar, J. *Photochem. Photobiol.* **1978**, *169*−*173*, 28.
(37) Dudley, K. H.; Ehrenberg, A.; Hemmerich, P.; Müller, F. *Helv. Chim. Acta* **1964**, *47*, 1354.
(38) Stanley, R. J.; Jang, H. *J. Phys. Chem. A* **1999**, *103*, 8976.
(39) Salomon, M.; Christie, J. M.; Knieb, E.; Lempert, U.; Briggs, W. R. *Biochemistry* **2000**, *39*, 9401.
(40) Abe, M.; Kyogoku, Y.; Kitagawa, T. *Spectrochim. Acta, Part A* **1986**, *42*, 1059.
(41) Sakai, M.; Takahashi, H. *J. Mol. Struct. (THEOCHEM)* **1996**, *379*, 9.
(42) Melø, T. B.; Ionescu, M. A.; Haggquist, G. W.; Naqvi, K. R. *Spectrochim. Acta, Part A* **1999**, *55*, 2299.
(43) *Gaussian 98 release notes*, revision A.11.2; Gaussian, Inc.: Pittsburg, PA, 2002.
(44) Kottke, T. Unpublished results.